Method for measuring small optical absorption coefficients with use of a Shack–Hartmann wave-front detector

Sanichiro Yoshida, David H. Reitze, David B. Tanner, and Justin D. Mansell

We present a method for measuring absorption at the 1×10^{-5} cm^{-1} level in high-quality optical materials. Using a Shack–Hartmann wave-front detector, thermal lensing in these materials may be measured. Then, the absorption coefficient may be estimated by fitting the observed deformation to a thermal lensing model based on the temperature dependences of the refractive index and the thermal expansion coefficient. For a particular sample of fused silica, the absorption coefficient was determined to be $1.8 \pm 0.4 \times 10^{-5}$ cm^{-1}. Obtaining this result requires a resolution in the optical path length better than ± 0.1 nm. © 2003 Optical Society of America

OCIS codes: 350.6830, 160.6030, 160.4670, 260.3060.

1. Introduction

There are many important optical systems where beam-quality requirements are sufficiently stringent that thermally generated wave-front distortion becomes an issue. As an example, low-absorption fused silica is used for the transmissive optics in laser-based gravitational wave detectors (GWD).[1] These GWDs are designed to detect a strain of space-time on the order of 10^{-23}; the strain appears as a phase difference in the light traveling in the two 4-km-length arms of a Michelson interferometer. To enhance the signal-to-noise ratio, each interferometer arm is configured as an optical resonator; in addition, a power-recycling mirror located between the laser and the beam splitter returns the light reflected from the interferometer back into it. Thus both the beam splitter and the input mirrors of the arm resonators are exposed to continuous high transmitted power. Optical absorption in the substrates of these optics induces a spatial variation in their refractive indices, making them behave as lenses. This effect, known as thermal lensing,[2] changes the radius of curvature of the circulating light, reducing the power coupling into the interferometer and degrading the GWD's performance.[3]

Fused silica has quite low absorption at 1.06 μm, the wavelength of the Nd:YAG laser used in GWDs. Therefore it is suitable for the material of the transmissive optics of these interferometers. However, because precise phase control of the circulating light is crucial for high performance of the GWDs, it is important to quantify the absorption coefficient of each optic individually so that the thermal effect can be calculated accurately. There are several known methods to estimate the absorption coefficient in low-absorption materials. Boccara[4] estimated the absorption of a fused silica by measuring the deflection that a probe beam suffers when it passes through the thermal lens caused by 1.06-μm laser radiation. The key to successful measurement of the deflection by use of this method is an appropriate management of the spatial jitter (beam wandering) of the probe beam. Bunimovich *et al.*[5] employed laser calorimetry to estimate the absorption coefficient of fused-silica fibers. They measured the temporal variation of the sample temperature caused by turning on and off the heating laser and estimated the absorption coefficient from the thermal-rise and decay. Making use of the difference in the slope of the thermal rise,

S. Yoshida (syoshida@selu.edu) is with the Laser Interferometer Gravitational-Wave Observatory—Livingston, 19100 Ligo Lane, P.O. Box 940, Livingston, Louisiana 70754 and with the Department of Chemistry and Physics, Southeastern Louisiana University, SLU 10878, Hammond, Louisiana 70433. D. H. Reitze and D. B. Tanner are with the Department of Physics, University of Florida, P.O. Box 18440, Gainesville, Florida 32611. J. D. Mansell is with Intellite, Inc., 1717 Louisiana, Suite 202, NE, Albuquerque, New Mexico 87110.

Received 28 January 2003; revised manuscript received 16 May 2003.

0003-6935/03/244835-06$15.00/0

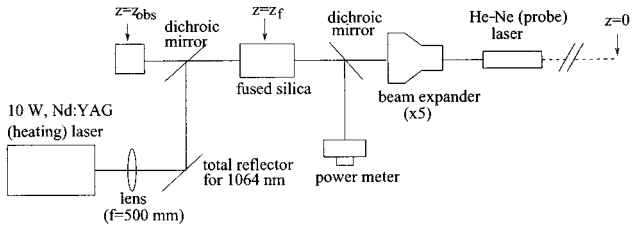

Fig. 1. Experimental setup. Dichroic mirrors are highly reflective at 1.06 μm and partially transmissive at 633 nm. $z = 0$ is the waist location of the probe beam. $z = z_f = 4.62$ m, and $z = z_{\mathrm{obs}} = 4.84$ m denote the locations of the sample and the image plane of the SHWD, respectively.

they separated the absorption coefficient of the surface from that of the bulk.[6]

In this paper we present a method for measuring absorption in high-quality, low-absorption optical materials. We use a Shack-Hartmann wave-front detector (SHWD, manufactured by WaveFront Sciences, Inc., Albuquerque, N. Mex.)[7] to measure the thermal lens due to high-power (10-W, cw) laser radiation.[8] To cope with very low absorption, we have developed a method for reducing noise associated with laser intensity fluctuation and spatial jitter. By fitting the spatial profile of the measured thermal lens to a model for thermal deformation, we were able to measure an absorption coefficient of $1.8 \pm 0.4 \times 10^{-5}$ cm^{-1} in a 2.5-cm-long sample of fused silica. This method is suitable for applications where the overall temperature rise of a massive sample is negligibly small but the temperature gradient is enough to cause thermal lensing.

Figure 1 illustrates our method. The fused-silica sample (Suprasil, manufactured by Heraeus, Hanau, Germany) used in this measurement was a cylinder 2.5 cm in diameter and 2.5 cm long. We exposed the sample to 10-W radiation from a cw Nd:YAG laser (Lightwave, model 220-1064-10000) operating in the TEM_{00} mode (the "heating beam"), and probed the thermally induced optical path length change ΔOPL by a He–Ne laser (the "probe beam"). The heating beam and the probe beam propagated in opposite directions through the sample.

Figure 2 illustrates the operation of the SHWD. The SHWD consists of a two-dimensional array of 20×20 lenslets mounted in front of a CCD. The diameter and the focal length of the lenslets in the SHWD used in this measurement are 0.25 and 25 mm, respectively. Each lenslet focuses the part of the probe beam incident on it onto the CCD. The specific CCD element on which the focal spot sits depends on the angle with which the probe beam enters the lenslet. The position of the focal point can be estimated accurately by the centroid algorithm.[7] The SHWD reconstructs the wave front by integrating the tilt over all the lenslets. Because each tilt represents ΔOPL over the diameter of the corresponding lenslet (Fig. 3), the reconstructed wave front represents ΔOPL for the entire probe beam as a function of the lateral location (r, θ), and can therefore be used to determine the thermal lens. Here (r, θ) are the polar coordinates on the cross-sectional plane of the sample. $\Delta OPL(r, \theta)$ is then averaged with respect to θ and the spatial profile of the thermal lens is evaluated as a function of r.

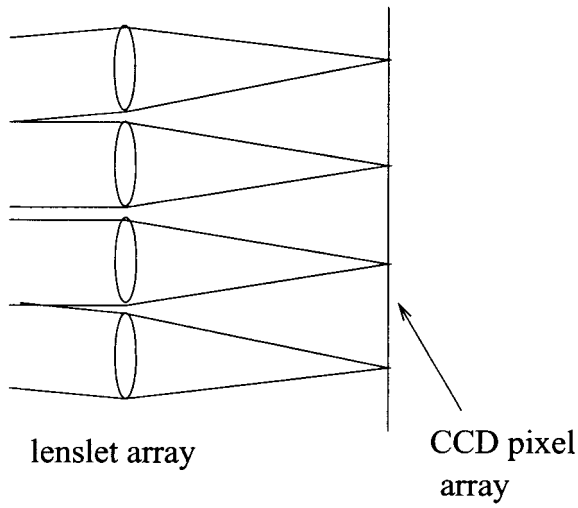

Fig. 2. Schematic view of lenslet and detector arrays in the SHWD.

When a Gaussian beam goes through an optic, a thermal lens is formed by the following mechanism: The radial intensity profile of the Gaussian beam induces a temperature gradient, causing spatial variation of both the refractive index and the physical length, on account of the temperature variations of these quantities. Assuming that the sample is much larger than the heating beam and that absorption is uniform in the sample, the steady-state, radial temperature distribution is given by[2,8]

$$\Delta T(r) = \frac{P\gamma l}{4\pi\kappa}\left[\sum_{i=0}^{\infty}\frac{(-1)^i\left(2\,\dfrac{r^2}{w^2}\right)^i}{ii!}\right], \qquad (1)$$

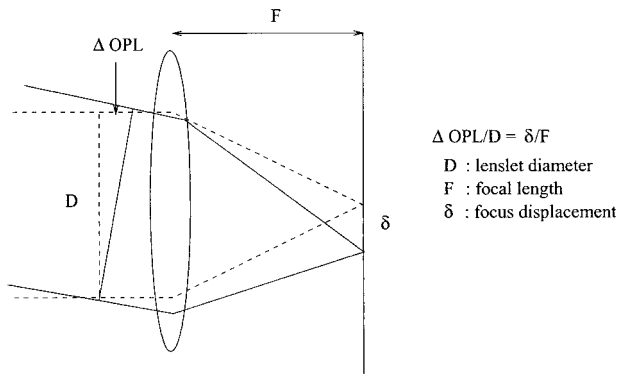

Fig. 3. Schematic view of the relationship between the displacement of focal point on the detector plane (δ) and the change in the wavelength slope. The dashed curve represents the reference wavefront and the solid line represents the data wave front.

where ΔT is the relative temperature at radius r (referenced to the center of the Gaussian profile), P is the laser power, γ is the absorption coefficient, l is the sample length along the beam path, and κ is the thermal conductivity. Using an empirically derived approximation, the change in optical path difference ΔOPL as a function of the radius becomes

$$\Delta OPL = 0.07741 \frac{P\gamma l}{\kappa}\left(\frac{\mathrm{d}n}{\mathrm{d}T} + \alpha n\right) \times \left[\left(\frac{r}{w}\right)^2 + 0.4\left(\frac{r}{w}\right)\right], \tag{2}$$

where n is the index of refraction, T is the temperature, α is the thermal expansion coefficient, and w is the spot size of the heating beam. This approximation is applicable only for the case $r < w$.

For thermal lens measurements, the SHWD is usually used in the following way. First, an image file is taken with the probe beam transmitted through the sample without exposing it to the heating beam. The positions on the CCD plane of the focal points from all of the lenslets are determined by the centroid algorithm. These focal positions are called the reference centroids, and the file containing the reference centroids is called the reference file. Next, the heating beam is superposed on the probe beam collinearly, keeping all the optics in the probe beam path unchanged.[8] The centroids (called the data centroids) are determined in the same way. Then by comparing data centroids and the reference centroids for the respective lenslets, the displacements of the focal positions are calculated. From these displacements the changes in the slope of the wave front (called the tilts) are calculated for the respective lenslets.

In our case, some extra arrangements were needed to cope with the extremely small absorption and the corresponding small thermal lens. First, we optimized the heating beam size relative to the probe laser beam size. Because $\Delta OPL(r)$ varies as a function of r/w where w is the spot size of the heating beam [see Eq. (2)], ΔOPL/lenslet increases as the heating beam size decreases relative to the probe beam size. (In other words, as the heating beam size decreases relative to the lenslet size on the object plane, each lenslet sees a larger portion of the thermal lens.) Therefore, to enhance the tilt per lenslet, it is desirable to reduce the size of the heating beam relative to the probe beam. However, if the heating beam size is too small, the total number of lenslets involved in the whole thermal lens diameter becomes too small, resulting in considerably lower spatial resolution. Thus there are optimum values for the sizes of both beams. We set the spot sizes of the heating beam and the probe beam at the sample location to be 0.7 and 2.5 mm, respectively. We optimized these values empirically. The Gaussian probe beam was large enough to provide fairly uniform illumination over the entire pump beam.

Second, we collimated the probe laser so that its wave front was as flat as possible, and adjusted the probe laser intensity as high as allowed by the linear range of the CCD. When the probe wave front is flat, the reference centroid is located close to the center of the lenslet. In this way, the influence of lenslet-to-lenslet optical crosstalk[7] can be greatly reduced. Also, by increasing the intensity, the precision of intensity digitization to 256 (8-bit) gray levels is increased; hence, the accuracy of the numerical operation increases.

Third, to get good signal-to-noise ratio, we used averaging both of angle θ and of the results of several runs. In addition, we made measurement both with and without the heating beam on to allow for variations in the probe beam. With the size of the thermal lens in this measurement, the tilt caused by spatial jitter (beam wandering) of the probe laser is not negligible. Consequently, if the above-mentioned usual procedure is taken, the reconstructed wave fronts are different from run to run. To overcome this problem, we adopted the following procedure: (1) Make a reference file as usual. (2) Make N additional measurements without applying the heating beam, N is typically 10 but can be as large as necessary to get a satisfactory signal-to-noise ratio. (3) Calculate the tilts for each of these N measurements using the reference file made in step (1). (4) Take an average of the resultant N data sets. (5) Reconstruct a wave front from the average of the N data sets made in step (4). (6) Evaluate the spatial profile $\Delta OPL(r)$ by averaging $\Delta OPL(r, \theta)$ with respect to θ. [The resultant $\Delta OPL(r)$ is called the 0-W data.] The measured center of the probe beam is chosen to be the center of the polar coordinate system when this average is made. Then, (7) expose the sample to the 10-W heating beam, make N measurements, and repeat steps (3)–(6) using the same reference file as the 0-W data. [The resultant $\Delta OPL(r)$ is called the 10-W data.] Finally, (8) subtract the 0-W data from the 10-W data to evaluate the thermal lens as a function of r. In this work we used a modal wave-front reconstruction based on a second-order Cartesian polynomial[9] in step (5). When $\Delta OPL(r, \theta)$ is averaged over θ in step (6) we approximate the integration along the circumference at a constant r by summation over square pixels having a finite width. Therefore as r decreases the quantization error becomes larger. In addition, the slope of $\Delta OPL(r)$ decreases as $1/r$, making the extracted tilt more vulnerable to unavoidable noise such as electric noise. In the analysis below, we discard $\Delta OPL(r)$ data obtained in the range of $r/w < 0.2$.

The jitter that the probe laser experiences during the acquisition of N data sets is reduced by this averaging, reducing the run-to-run variation in $\Delta OPL(r)$. The resultant averaged 0- and 10-W data still contain the influence of the jitter that the probe laser suffers at the moment when the image for the reference file is taken. However, because both the 0-W and 10-W data are based on the same reference

Table 1. Numbers Used to Estimate the Absorption Coefficient

$\frac{dn}{dT}\left(\frac{1}{K}\right)$	$\alpha\left(\frac{1}{K}\right)$	n	l (cm)	$\kappa\left(\frac{W}{mK}\right)$
9.8×10^{-6}	5.1×10^{-7}	1.45	2.5	1.38

file, this influence is removed when the 0-W data is subtracted from the 10-W data in step (8).

Once the spatial profile of the wave front is obtained, the absorption coefficient can be calculated by fitting the profile to Eq. (2). Provided that all of the other constants are known, the absorption coefficient can be estimated by fitting the measured thermal lens profile to the theoretical profile calculated by Eq. (2) with use of the absorption coefficient γ as the fitting parameter. We estimated the absorption coefficient in this fashion. Table 1 lists the numbers we used for this calculation.[10]

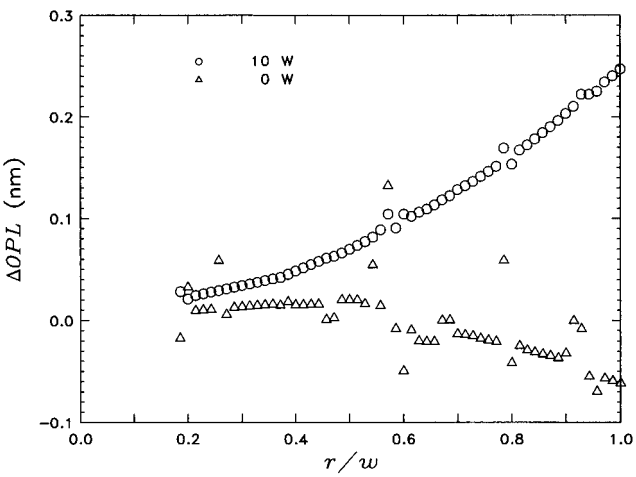

Fig. 4. Sample 10-W and 0-W data.

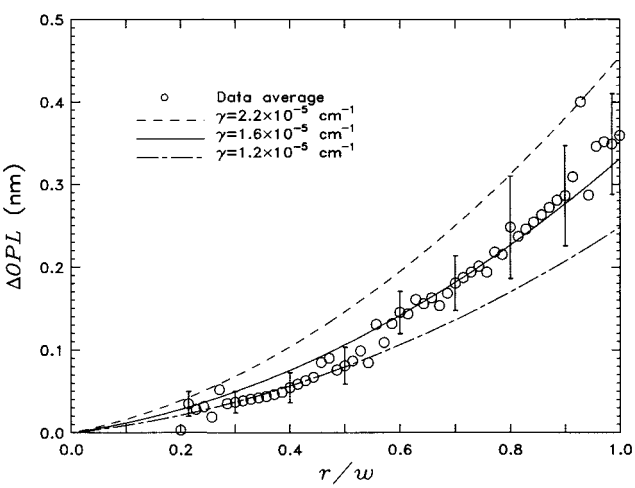

Fig. 5. The points are the averaged wave front at 10 W. The lower dotted curve shows the calculated wave front for an absorption coefficient of 1.2×10^{-5} cm^{-1}; the upper dotted curve is for 2.2×10^{-5} cm^{-1}.

Figure 4 shows an example of 10-W data as a function of r/w, together with the corresponding 0-W data. The deviation of the 0-W data from the horizontal axis [i.e., the line corresponding to $\Delta OPL(r) = 0$] indicates the influence of the probe beam's jitter on the reference measurement. The increase in deviation toward the edge of the beam illustrates the larger influence of the jitter at the edge (because the wave front tilts more near the edge).

We repeated these measurements five times. All of the resultant $\Delta OPL(r)$ fall between the theoretical curves calculated from Eq. (2) for absorption coefficients of 1.2×10^{-5} cm^{-1} and 2.2×10^{-5} cm^{-1}. Figure 5 shows $\Delta OPL(r)$ averaged over all of these data, where the two dotted curves are theoretical values corresponding to these limiting values of the absorption coefficient. After the averaging, the measured data best fits to a theoretical curve corresponding to an absorption coefficient of $1.64 \pm 0.32 \times 10^{-5}$ cm^{-1}. To assess the level of possible thermal lensing by the dichroic mirror, we measured $\Delta OPL(r)$ without having a fused-silica sample in the setup shown in Fig. 1. No $\Delta OPL(r)$ was observed, indicating that the thermal lensing effect in the dichroic mirror is negligible.

The $\Delta OPL(r)$ shown in Fig. 5 represents the change in the wave-front curvature observed at the image plane of the SHWD. In contrast, thermal lensing in the fused-silica sample causes a change in the wave-front curvature at the location where the sample is placed. In general, when a lens is placed on the optical path of a Gaussian beam, the resultant change in the wave-front curvature depends on where it is observed, because the beam diverges as it propagates. In our setup, we needed to place the dichroic mirror between the sample and the SHWD (Fig. 1). Therefore there is a finite distance between the observation point and the sample location, making the optical path length change observed by the SHWD not strictly the same as the optical path length change caused by the thermal lensing. We now assess the correction associated with this fact.

To make this assessment simpler, we approximate the thermal lens by a spherical lens of focal length f and place it in the optical path of a Gaussian beam. Although the thermal lens is not exactly a spherical lens, as indicated by Eq. (2), this approximation will be adequate for this assessment. We have calculated the overlap integral to estimate the intensity coupled into higher-order Gaussian modes by the nonspherical term of a thermal lens represented by Eq. (2). According to this calculation, the intensity in these modes for our observed $\Delta OPL(r)$ is less than 0.1%.

Suppose now that the Gaussian beam has its waist at $z = 0$ and that the lens and the SHWD are placed at $z = z_f$ and $z = z_{obs}$, respectively. By considering the propagation of Gaussian beams and using ray

matrices,[11] the radius of curvature at $z = z_{\mathrm{obs}}$ of the probe beam, $R_{\mathrm{obs}}{}^{10W}$, can be written as follows:

$$R_{\mathrm{obs}}{}^{10W} = \frac{\left\{\left(\frac{1}{R_f} - \frac{1}{f}\right)\left[1 + \Delta z\left(\frac{1}{R_f} - \frac{1}{f}\right)\right] + \Delta z\left(\frac{\lambda}{\pi w_f{}^2}\right)^2\right\}^2 + \left(\frac{\lambda}{\pi w_f{}^2}\right)^2}{\left[\left(\frac{1}{R_f} - \frac{1}{f}\right)^2 + \left(\frac{\lambda}{\pi w_f{}^2}\right)^2\right]\left\{\left(\frac{1}{R_f} - \frac{1}{f}\right)\left[1 + \Delta z\left(\frac{1}{R_f} - \frac{1}{f}\right)\right] + \Delta z\left(\frac{\lambda}{\pi w_f{}^2}\right)^2\right\}}, \tag{3}$$

where R_f is the radius of curvature incident to the lens, λ is the wavelength of the probe laser, w_f is the spot size of the probe beam at the lens, f represents the focal length of the thermal lens, and Δz is the distance between the lens and observation point. When the heating beam is absent, the probe laser's curvature at $z = z_{\mathrm{obs}}$ is

$$R_{\mathrm{obs}}{}^{0W} = \frac{\left[\frac{1}{R_f}\left(1 + \frac{\Delta z}{R_f}\right) + \Delta z\left(\frac{\lambda}{\pi w_f{}^2}\right)^2\right]^2 + \left(\frac{\lambda}{\pi w_f{}^2}\right)^2}{\left[\left(\frac{1}{R_f}\right)^2 + \left(\frac{\lambda}{\pi w_f{}^2}\right)^2\right]\left[\frac{1}{R_f}\left(1 + \frac{\Delta z}{R_f}\right) + \Delta z\left(\frac{\lambda}{\pi w_f{}^2}\right)^2\right]}. \tag{4}$$

The optical path length change measured by the SHWD at $z = z_{\mathrm{obs}}$, $\Delta OPL_{\mathrm{obs}}$, is proportional to the difference between $1/R_{\mathrm{obs}}{}^{0W}$ and $1/R_{\mathrm{obs}}{}^{10W}$

$$\Delta OPL_{\mathrm{obs}} \propto \frac{1}{f_{\mathrm{eff}}} = \frac{1}{R_{\mathrm{obs}}{}^{0W}} - \frac{1}{R_{\mathrm{obs}}{}^{10W}}, \tag{5}$$

where f_{eff} indicates the effective focal length evaluated at $z = z_{\mathrm{obs}}$ by Eq. (5). Then the question becomes how f_{eff} is different from the true f. From Fig. 5 and the spot size of the heating beam at the thermal lens, f_{eff} of this measurement can be estimated to be 670 m. From an analysis of the reference file, we estimate that the probe laser has a waist of 0.348 mm at a position 4.62 m away from the fused silica sample (Fig. 1). From these numbers together with $\Delta z = 0.22$ m, and using Eqs. (3)–(5), we can explore which value of f gives the closest number to the measured f_{eff} of 670 m. When f is 612 m, f_{eff} calculated by Eq. (5) is closest to the measured value of 670 m, indicating that the focal length evaluated at $z = z_{\mathrm{obs}}$ is 9.6% larger than the true focal length at $z = z_f$. In fact, our calculation indicates that this error factor is fairly insensitive to the value of f, varying from 9.4 to 9.6%, whereas f varies from 100 to 1000 m. Therefore it is reasonable to use the error factor of 9.6% for the above-mentioned absorption coefficient corresponding to the best-fit ΔOPL, and estimate the corrected absorption coefficient to be $1.8 \pm 0.35 \times 10^{-5}$ cm^{-1}. This absorption coefficient is approximately 20% higher than the value of 1.51×10^{-5} cm^{-1} that Boccara[4] estimated by beam deflection technique on samples of the same material. It is 2 orders of magnitude smaller than the absorption coefficient estimated by Bunimovich *et al.*[5] for a fused-silica fiber.

Finally, we briefly discuss the meaning of the ΔOPL in these measurements. In Figs. 4 and 5, the resolution of this measurement appears to be better than 0.1 nm, which corresponds to a wave-front slope of 0.1 nm/250 μm = 4×10^{-7} rad. This value is 1 order of magnitude better than the resolution estimated for a similar wave-front measurement with use of the same type of SHWD,[7] where the authors claim that the limiting factors for the resolution are sensor noise and lenslet-to-lenslet optical crosstalk. We believe that in our case the above-mentioned optimization of the wave front and intensity of the probe laser reduces the optical crosstalk greatly. According to a numerical calculation made by Armstrong,[12] the wave-front slope of 4×10^{-7} (rad) corresponds to a theoretical rms centroid error owing to pure electrical amplitude noise (gain variation in pixels) when an error of 0.1% of the maximum amplitude is assumed. It seems that the averaging procedure we employed contributes to reduction of the electrical noise.

Unlike the calorimetric approach employed by Bunimovich *et al.*,[6] our method cannot separate the surface absorption from the bulk absorption in a single measurement. However, as Eq. (2) indicates, the contribution of surface absorption to the measured ΔOPL is proportional to the product of the absorption coefficient and the thickness of the surface layer. Therefore, unless the absorption coefficient of the surface layer is much larger than the bulk or the bulk length is comparable with the surface thickness, surface absorption gives a much smaller thermal lens than bulk absorption. In the case of the fused-silica transmissive optics used in the above-mentioned GWDs, the surface absorption is 2 orders of magnitude lower than the bulk absorption.[13] If it were necessary to separate the surface absorption, we can prepare two samples having the same surface conditions and different bulk length. Then the bulk absorption can be estimated from the difference in ΔOPL of the two samples.

In summary, we have demonstrated a measurement of very low absorption in fused silica using a Shack–Hartmann wave-front detector to measure the properties of a thermal lens introduced by a 10-W, 1.06-μm wavelength laser. By adjusting the beam shape and intensity of the probe laser appropriately and by averaging the acquired image data, we have

been able to measure ΔOPL on the order of 10^{-10} m. From the measured ΔOPL we have estimated the absorption coefficient of the fused silica sample to be $1.8 \pm 0.4 \times 10^{-5}$ cm^{-1}.

We thank Q. Shu for his helpful discussion on the data correction associated with the divergence of the probe beam. This work was supported by the National Science Foundation through grants PHY-0070854 and PHY-9900786.

References

1. A. Abramovici, W. Althouse, R. W. P. Drever, Y. Gursel, S. Kawamura, F. J. Raab, D. Shoemaker, L. Sievers, R. E. Spero, K. Thorne, R. E. Vogt, R. Weiss, S. E. Whitcomb, and M. E. Zucker, "The Laser Interferometer Gravitational-wave Observatory," Science **256,** 325–333 (1992).
2. K. Strain, K. Danzmann, J. Mizuno, P. Nelson, A. Rüdiger, R. Schilling, and W. Winkler, "Thermal lensing in recycling interferometric gravitational wave detectors," Phys. Lett. A. **194,** 124–132 (1994).
3. D. E. McClelland, J. B. Camp, J. Mason, W. Kells, and S. E. Whitcomb, "Arm cavity resonant sideband control for laser interferometric gravitational wave detectors," Opt. Lett. **24,** 1014–1016 (1999).
4. Claude Boccara, Laboratoire d'Optique Physique, Paris, France (private communication, 1998).
5. D. Bunimovich, E. Belotserkovsky, L. Nagli, and A. Katzir, "Measurements of absorption coefficients using noncontact fiber-optic laser calorimetry," Appl. Opt. **34,** 743–745 (1995).
6. D. Bunimovich, L. Nagli, and A. Katzir, "Absorption measurements of mixed silver halide crystals and fibers by laser calorimetry," Appl. Opt. **33,** 117–119 (1994).
7. D. R. Neal, D. J. Armstrong, and W. T. Turner, "Wavefront sensors for control and processing monitoring in optics manufacture," in *Laser as Tool for Manufacturing II*, L. R. Migliore and R. D. Schaeffer, eds., Proc. SPIE **2993,** 211–220 (1997).
8. J. D. Mansell, J. Hennawi, and E. K. Gustafson, "Evaluating the effect of transmissive optic thermal lensing on laser beam quality with a Shack–Hartmann wave-front sensor," Appl. Opt. **40,** 366–374 (2001).
9. *CLAS2D Operation Manual, Revision 1.50a* (WaveFront Sciences, Inc., Albuquerque, N. Mex., 1999), p. 69.
10. *Quartz Glass for Optics, Optical Properties* (Heraeus, Hanau, Germany, 1994).
11. See for example, A Yariv, *Introduction to Optical Electronics* (Holt, Rinehart and Winston, New York, 1976), chaps. 2 and 3.
12. Darren Armstrong, WaveFront Sciences, Inc., 14810 Central Avenue NW, Albuquerque, N. Mex. 87123-3905 (private communication, 1998).
13. R. Beausoleil, Edward L. Ginzton Laboratory Stanford University, Stanford, Calif. 94305 (private communication, 2000).